Algebraic Hastatic Order in One-Dimensional Two-Channel Kondo Lattice

Milan Kornjača and Rebecca Flint
Ames National Laboratory, U.S. Department of Energy, Ames, Iowa 50011, USA
and Department of Physics and Astronomy, Iowa State University, 12 Physics Hall, Ames, Iowa 50011, USA

(Received 22 March 2023; accepted 4 June 2024; published 11 July 2024)

The two-channel Kondo lattice likely hosts a rich array of phases, including hastatic order, a channel symmetry breaking heavy Fermi liquid. We revisit its one-dimensional phase diagram using density matrix renormalization group and, in contrast to previous work, find algebraic hastatic orders generically for stronger couplings. These are heavy Tomonaga-Luttinger liquids with nonanalyticities at Fermi vectors captured by hastatic density waves. We also find a predicted additional nonlocal order parameter due to interference between hastatic spinors, not present at large N, and residual repulsive interactions at strong coupling suggesting non-Fermi-liquid physics in higher dimensions.

DOI: 10.1103/PhysRevLett.133.026503

The Kondo lattice model is a foundational model of correlated electron physics, capturing how antiferromagnetic (AFM) interactions between conduction electrons and local moments lead to heavy Fermi liquids, where the spins are incorporated into the Fermi surface. The model can be solved analytically in a large-N limit, which captures the heavy Fermi liquid [1,2], with $1/N$ corrections leading to magnetic order, quantum criticality, and superconductivity [3–6]; numerical results in one dimension (1D) are largely consistent with large-N, finding a heavy Tomonaga Luttinger liquid (TLL) [7–16] apparently stabilized by magnetic fluctuations [17]. The two-channel Kondo lattice is a well-studied extension, with two symmetry-related conduction electron channels. The impurity is quantum critical [18–20], with a residual Majorana fermion. The lattice has a rich interplay of spin and channel, and Majorana signatures may survive to higher dimensions [21–23]. The model can be solved in two large-N limits, leading to composite pair superconductivity [24–26] for SP(N) and channel symmetry breaking heavy Fermi liquids known as hastatic order for SU(N) [27–34]. The physical $N = 2$ limit has been studied numerically in 1D [35,36] and infinite dimensions [21,26,28–30,37,38], but many questions remain, including the general phase diagram; validity of large-N limits, including the presence of composite pair superconductivity; and the nature and Fermi wave vectors of metallic phases, including non-Fermi-liquid signatures.

Given recent analytical insights [27,31,32,39] and computational improvements, we revisit the 1D two-channel Kondo lattice using density matrix renormalization group (DMRG). We can now address both potential order parameters and Luttinger liquid properties, including whether there are "heavy" TLLs. Our results are summarized in Fig. 1. We find algebraic hastatic order at larger couplings for all conduction electron fillings except half filling, and we find these are heavy TLLs incorporating the spins into the Fermi surface. Surprisingly, the two-channel combination of channel and magnetic fluctuations appears

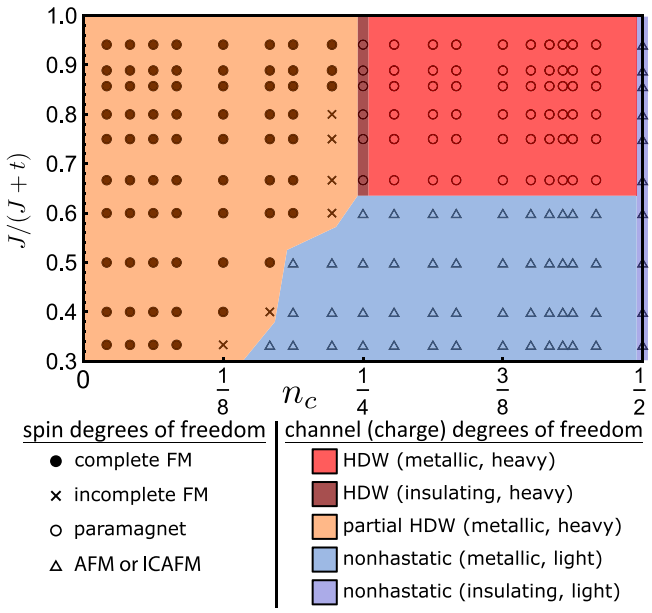

FIG. 1. Zero temperature phase diagram of the 1D two-channel Kondo lattice obtained with DMRG, as a function of conduction electron filling (n_c) and Kondo coupling (J). The ground state has magnetic and channel or hastatic orders, denoted by symbols and colors as described in the legend. Regions are "heavy," incorporating at least some spins into the Fermi sea, or "light." Quarter and half filling are commensurate hastatic density wave (HDW) and antiferromagnetic (AFM) insulators, respectively, while all other regions are metallic with generically incommensurate orders. There are three distinct metallic regions: a coexisting ferromagnet and HDW (FMHDW) for $n_c < 1/4$, where n_c spins are screened and the rest order ferromagnetically; a pure HDW for stronger coupling and $1/4 < n_c < 1/2$; and a weak-coupling AFM without hastatic correlations (ICAFM).

to be more effective in stabilizing the heavy TLL than the one-channel model [17]. Our study greatly extends previous results [36], which found algebraic hastatic order only at quarter filling and did not examine the nature of the metallic phases. Our results have implications for non-Kramers doublet materials, where two-channel Kondo physics may be relevant for unconventional superconductivity in UBe_{13} [21,37,40,41], 1-2-20 Pr-based materials physics [22,31,42–44], and hidden order in URu_2Si_2 [27,39,45].

The 1D two-channel Kondo lattice model is

$$H = -t\sum_{i\alpha\sigma} c^\dagger_{i\alpha\sigma} c_{i+1\alpha\sigma} + \text{H.c.} + \frac{J}{2}\sum_{i\alpha\sigma\sigma'} \mathbf{S}_{fi}\cdot c^\dagger_{i\alpha\sigma}\boldsymbol{\sigma}_{\sigma\sigma'} c_{i\alpha\sigma'}, \quad (1)$$

where $t = 1$ is the conduction electron hopping and $J > 0$ is the Kondo coupling. i labels sites ($1 \le i \le L$), where each site has both conduction electrons ($c^\dagger_{i\alpha\sigma}$) with spin σ and channel α, and local $S = 1/2$ moments ($\mathbf{S}_{fi}$). $\boldsymbol{\sigma}$ are the Pauli matrices in spin space. We fix the conduction electron filling, $0 \le n_c \le 1$, with $n_c = 1$ indicating four electrons per site. This is the simplest Kondo model with both SU(2) spin and SU(2) channel symmetries.

The channel degeneracy leads to a rich possibility of phases. These can be divided into "heavy" and "light" phases, where the spins are either incorporated into the Fermi sea or remain decoupled; in the light phases these typically order magnetically, $\langle \mathbf{S}_{fi}\rangle \neq 0$. There are two proposed heavy orders: a channel symmetry breaking heavy Fermi liquid that we call hastatic order [27,28], and composite pair superconductivity [24], which incorporates the spins directly into heavy Cooper pairs. These orders arise within different large-N limits of the SU(2) two-channel model, where the more commonly used SU(N) limit leads to hastatic order, and composite pairing arises in the symplectic-N limit extending SU(2) to SP(N) [25]. For $N = 2$ and $n_c = 1/2$, these are components of an SO(5) composite order parameter. Both have been found in $d = \infty$ away from half filling [26,28–30], and both form either uniform or modulated orders.

The hastatic order parameter, $\vec{\Psi}$, is a composite order parameter of conduction and f moments that captures the Kondo singlet channel polarization:

$$\boldsymbol{\Psi}(i) = \frac{1}{2}\sum_{\sigma\sigma'\alpha\alpha'} c^\dagger_{i\alpha\sigma}\boldsymbol{\sigma}_{\sigma\sigma'}\boldsymbol{\tau}_{\alpha\alpha'} c_{i\alpha'\sigma'}\cdot\mathbf{S}_{fi}, \quad (2)$$

where $\boldsymbol{\tau}$ are channel Pauli matrices. The $\hat{z}$ component is manifestly channel polarization, $\Psi^z(i) = (\mathbf{S}_{ci,\alpha=+} - \mathbf{S}_{ci,\alpha=-})\cdot\mathbf{S}_{fi}$ [28]. Hastatic order also generates staggered channel polarization in the conduction electrons, $n_{i\alpha\sigma} = c^\dagger_{i\alpha\sigma}c_{i\alpha\sigma}$, whose correlations were used previously [36].

The complex composite pair order parameter is

$$\Delta_{\text{CP}}(j) = \sum_{\alpha\sigma\sigma'} c^\dagger_{j\alpha\sigma'}[\boldsymbol{\sigma}(i\sigma_2)]_{\sigma\sigma'} c^\dagger_{j\bar{\alpha}\sigma'}\cdot\mathbf{S}_{fj}, \quad (3)$$

with $\bar{\alpha} = -\alpha$. Electrons in orthogonal channels screen the same spin, giving singlet superconductivity.

An additional hastatic order parameter was recently predicted [39]. In large N, hastatic order has a *spinorial* order parameter $\langle V_{i\alpha}\rangle$ representing a channel-dependent Kondo singlet. This quantity is gauge dependent, meaning finite-N order parameters must be bilinears. The composite order parameter, $\boldsymbol{\Psi}(i) \propto \sum_{\alpha\alpha'}\langle V^*_{i\alpha}\boldsymbol{\tau}_{\alpha\alpha'}V_{i\alpha'}\rangle$, is associated with the on-site moments of these spinors, but another, nonlocal order parameter can arise from interference between spinors at different sites, break additional symmetries [31,39]. This interference requires intersite spin correlations, and is not present for $N = \infty$. $1/N^2$ Ruderman–Kittel–Kasuya–Yosida couplings generate these correlations [46,47], often treated within large-N Kondo-Heisenberg models [31,47] as an emergent f hopping $t_{f,ij}$ describing spin-liquid physics. This order parameter, $\vec{\Phi}(i,j) \propto \sum_{\alpha\alpha'}\langle t_{f,ij}V^*_{i\alpha}\boldsymbol{\tau}_{\alpha\alpha'}V_{j\alpha'}\rangle$, is only present in modulated hastatic phases, and may be written as [39]

$$\Phi^a(i,j) = i\sum_{\sigma\sigma'\alpha\alpha'}\mathbf{S}_{f,i}\cdot\left(c^\dagger_{i\alpha\sigma}\tau^a_{\alpha\alpha'}\boldsymbol{\sigma}_{\sigma\sigma'}c_{j\alpha'\sigma'}\times\mathbf{S}_{f,j}\right), \quad (4)$$

where i, j denote the sites, typically nearest neighbors, whose spinorial interference generates $\vec{\Phi}$. The coexistence of a local, composite order parameter $\vec{\Psi}$ and a nonlocal, spin-liquid-like order parameter $\vec{\Phi}$ is reminiscent of the order parameter fragmentation found in spin ice [48–50], and is an explicit example of Kondo order parameter fractionalization [51,52].

We obtained the ground state phase diagram using finite system DMRG [53,54] in an ITensor implementation [55] with open boundary conditions. We conserve the total conduction electron number, $n_c = (1/4L)\sum_{i\alpha\sigma} n_{i\alpha\sigma}$, and the z component of total angular momentum, $S^z = \sum_i[S^z_{fi} + \sum_\alpha S^z_{ci\alpha}]$, where $\mathbf{S}_{ci\alpha} = \frac{1}{2}\sum_{\sigma\sigma'} c^\dagger_{i\alpha\sigma}\boldsymbol{\sigma}_{\sigma\sigma'}c_{i\alpha\sigma'}$ is the conduction electron spin for a given site and channel. We use bond dimensions of up to $m = 5000$ on lattices of up to $L = 96$ sites, resulting in a maximum discarded weight of 10^{-6} (with $<10^{-8}$ typical in the strong-coupling regions), implying generally good convergence. All figures used $L = 72$. The phase diagram shown in Fig. 1 was mapped out via ground state correlation functions in the lowest energy total spin sectors as a function of n_c, for $0 \le n_c \le 1/2$, and J, for $1/3 \le J/(J+t) \le 16/17$.

We examined the following correlation functions:

$$\begin{aligned} S_\Psi(x) &= \langle\Psi^z(i)\Psi^z(i+x)\rangle, \\ S_\Phi(x) &= \langle\Phi^z(i,i+1)\Phi^{z\dagger}(i+x,i+1+x)\rangle, \\ S_f(x) &= \langle S^z_{fi}S^z_{f,i+x}\rangle. \end{aligned} \quad (5)$$

The first measures composite order correlations, which captures the same physics as the conduction channel polarization correlations, $D(x) = \sum_{\sigma\sigma'\alpha\alpha'}\alpha\alpha'\langle n_{i\alpha\sigma}n_{i+x\alpha'\sigma'}\rangle$, used

previously [36]. $S_\Phi(x)$ captures correlations of the nearest-neighbor Φ order parameter, while $S_f(x)$ captures spin correlations. We fix the reference site $i = 10$, but results are unchanged by averaging over i's sufficiently far from the edges; x is a discrete variable representing distances between sites. We use the SU(2) symmetries to fix the spin or channel components to $\hat{z}$.

The peculiarities of 1D allow DMRG to efficiently study this model, but also mean there is no long-range order, only algebraic or exponential correlations, and Luttinger instead of Fermi liquids. The nature of these gapless phases is indicated by their central charge, which can be calculated via the scaling of entanglement entropy with system size cut [56,57], as shown in the Supplemental Material [58]; see also [59–62]. We find that all metallic hastatic density waves (HDWs) have central charge, $c = 2$, while the insulating quarter filled HDW has $c = 1$, as does the insulating half filled AFM. Integer central charge implies that all HDW regions are Tomonaga-Luttinger liquids, although how the charge, spin, and channel sectors contribute in the metallic HDWs is an open question. While TLLs do not have a jump at the Fermi wave vector, they have nonanalyticities at k_F that manifest in both spin and charge Friedel oscillations, whose Fourier transforms have peaks at $2k_F$ and $4k_F$ [8,9,17], as well as directly in the conduction electron momentum distribution [13,61,63]:

$$n_q = \frac{1}{L}\sum_{ij\alpha\sigma} e^{iq(i-j)}\langle c^\dagger_{i\alpha\sigma} c_{j\alpha\sigma}\rangle. \tag{6}$$

We sum over all i, j, but results are similar if sites near the edges are excluded, suggesting that our results represent bulk physics. We can now show that the HDW Fermi surfaces incorporate the spins [8,9,11–13,15,17,62,64,65], confirming a key large-N two-channel result [27,31–33]. We will show only n_q, which detects k_F directly, but the $2k_F$ and $4k_F$ Friedel oscillation peaks were used as checks [58]. The relative weight of these peaks and the overall spatial dependence of the Friedel oscillations can be used to extract the charge Luttinger parameter K, which contains information about residual interactions [9,17,61]. Note that TLLs have intrinsic algebraic spin, charge, and superconducting correlations, all with $1/x^\alpha$, $\alpha > 1$ power laws, while hastatic correlations, when present, dominate with $\alpha = 1$.

Now we turn to the nature of the five distinct ground states found in the phase diagram in Fig. 1. We confirm the spin correlations previously reported [36], but find additional hastatic correlations away from $n_c = 1/4$.

For low filling ($n_c < 1/4$) and moderate to strong coupling, there is a ferromagnetic region with coexisting algebraic hastatic order (FMHDW). n_c spins are screened by forming Kondo singlets, while the remaining spins are fully polarized with $S = S_{\max} = (1 - 4n_c)L/2$, analogous to the single-channel case [10,66], aside from a small incomplete ferromagnetic region near the phase boundary ($0 < S \leq S_{\max}$). Figure 2(b) shows the Ψ structure factor, $S_\Psi(q) = (1/L)\sum_x S_\Psi(x)e^{-iqx}$. The peak position gives the HDW Q vector, $Q = 4\pi n_c$, which approaches π at 1/4 filling. $S_\Psi(x)$ decays algebraically as $1/x$, while the spin correlations are those of a TLL. In Fig. 3(a), n_q has a nonanalyticity at $k_F^* = 2\pi n_c$, twice the light $k_F = \pi n_c$, indicating that n_c spins are incorporated into the Fermi surface. The total weight under $S_\Psi(q)$ depends on the number of screened spins, growing as n_c^2. While the FMHDW is a TLL, the charge Luttinger parameter $K(J)$ decreases with J, suggesting increasingly repulsive residual interactions as strong coupling is approached [58].

For $1/4 \leq n_c < 1/2$ and $J/(J + t) \geq 3/5$, there is a purely hastatic region (HDW), with fully screened spins

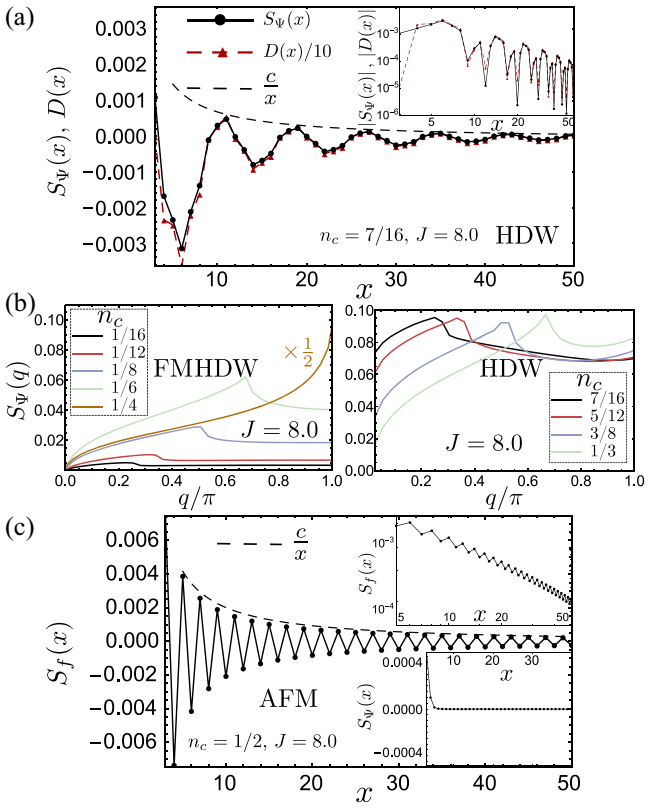

FIG. 2. (a) Example hastatic correlator $S_\Psi(x)$, with $n_c = 7/16$, $J = 8.0$. It decays algebraically, with a clear modulation. Note that $D(x)$ [36] closely follows $S_\Psi(x)$, up to a numerical factor. The inset log-log plot confirms the power-law decay. $S_\Psi(x)$ is similar for the FMHDW and HDW. (b) The Fourier transform $S_\Psi(q)$ for several n_c with $J = 8.0$. The Q obtained from the peak location smoothly evolves from nearly zero at low fillings to π at 1/4 filling as $Q = 4\pi n_c$ in the FMHDW (left); the weight under $S_\Psi(q) \propto n_c^2$, with the $n_c = 1/4$ curve reduced by 1/2. In the HDW ($n_c > 1/4$) (right), Q evolves smoothly from π as $Q = 4\pi(1/2 - n_c)$. (c) In the AFM insulator ($n_c = 1/2$), the spin correlator $S_f(x)$ has a $1/x$ power law (log-log plot in top inset), with $Q = \pi$, while $S_\Psi(x)$ (bottom inset) decays exponentially.

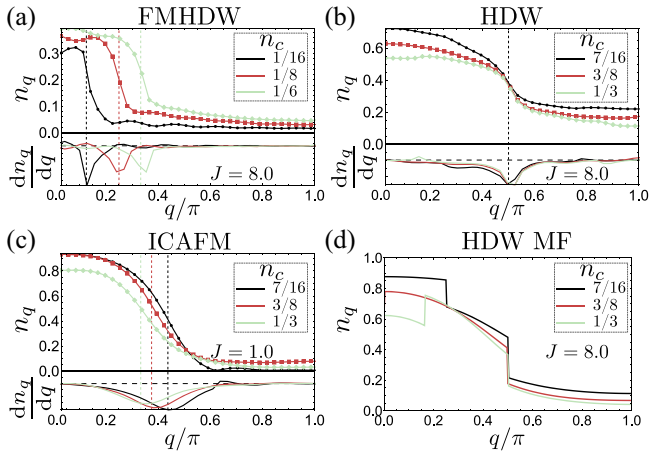

FIG. 3. For several n_c within each metallic region, we calculate the conduction electron momentum distribution n_q, which should have nonanalyticities at the Fermi wave vectors, with the derivative (dn_q/dq, arbitrary units) plotted below. The numerical results are in (a)–(c). Panel (a) shows the FMHDW n_q, with dashed lines indicating the nonanalyticity at $k_F^* = 2\pi n_c$, twice the light k_F, consistent with incorporating n_c spins into the Fermi sea. Panel (b) shows the HDW n_q, where the primary $k_F^* = \pi/2$, regardless of filling, with secondary n_c dependent nonanalyticities at lower q. Panel (c) shows n_q in the nonhastatic ICAFM, with light $k_F = \pi n_c$. In (d), we calculate n_q for the HDW within a large-N mean-field theory [58]. Only some heavy Fermi surfaces have nonzero *conduction* weight (n_q), including one pinned at $\pi/2$; the secondary nonanalyticity at low q is also qualitatively captured.

($S = 0$) and algebraic hastatic order at $Q = 4\pi(1/2 - n_c)$, with correlations again decaying as $1/x$. Exactly at $n_c = 1/4$, this is a hastatic Kondo insulator, with $Q = \pi$, and charge and spin gaps. Elsewhere, it is metallic—a heavy TLL, as seen in n_q in Fig. 3(b). The main nonanalyticity of n_q is pinned to $k_F^* = \pi/2$, regardless of filling. This pinning results from the Q dependence of n_c, and is captured within a large-N HDW mean-field theory [58]. The mean-field heavy bands are obtained at commensurate n_c, and the resulting conduction electron momentum distribution n_q is shown in Fig. 3(d). While there are many *heavy* band crossings, due to the large unit cell, we find typically only one or two Fermi surface jumps in n_q: one pinned to $k_F = \pi/2$ and an n_c dependent one at lower q. Both are consistent with DMRG results in location and sign [compare Figs. 3(b) and 3(d)].

At 1/2 filling, we find an AFM insulator, whose spin correlations decay as $1/x$ [Fig. 2(c)], with no spin gap. The hastatic correlations decay rapidly, suggesting the spins and conduction electrons are decoupled, although the electrons also have staggered algebraic spin correlations.

For weaker coupling, there is a nonhastatic, incommensurate antiferromagnet (ICAFM), where spins and conduction electrons have $Q = 2k_F = 2\pi n_c$, consistent with a spin-density wave of the light Fermi surface. n_q also shows this light $k_F = \pi n_c$, as seen by peaks in dn_q/dq in Fig. 3(c). Our results here are less reliable, as weak coupling ($J \lesssim 1.5$) is inherently harder to treat with DMRG, manifesting as higher maximum discarded weights. We therefore cannot conclusively calculate the central charge to confirm the proposed fractional central charge in the weak Kondo limit of the two-channel Kondo-Heisenberg model [33,60]. This region appears to have no charge or spin gaps and is reminiscent of the RKKY liquid phase hypothesized for $J \ll t$ in the single-channel lattice [11,17,36,67].

We also examined composite pair correlations, $S_{\mathrm{CP}}(x) = \langle \Delta_{\mathrm{CP}}(i)\Delta_{\mathrm{CP}}^{\dagger}(i+x)\rangle$, finding exponential suppression with generically short correlation lengths, by contrast to the algebraic TLL conventional superconducting correlations. In the HDW, $\Delta_{\mathrm{CP}}(i)$ is staggered, and the correlation length increases with J and n_c [58], consistent with the order found for $d = \infty$ [26].

Finally, we examine the additional hastatic order parameter $\vec{\Phi}$, which captures interference between neighboring hastatic spinors. $\vec{\Phi}$ has algebraic correlations in the HDWs,

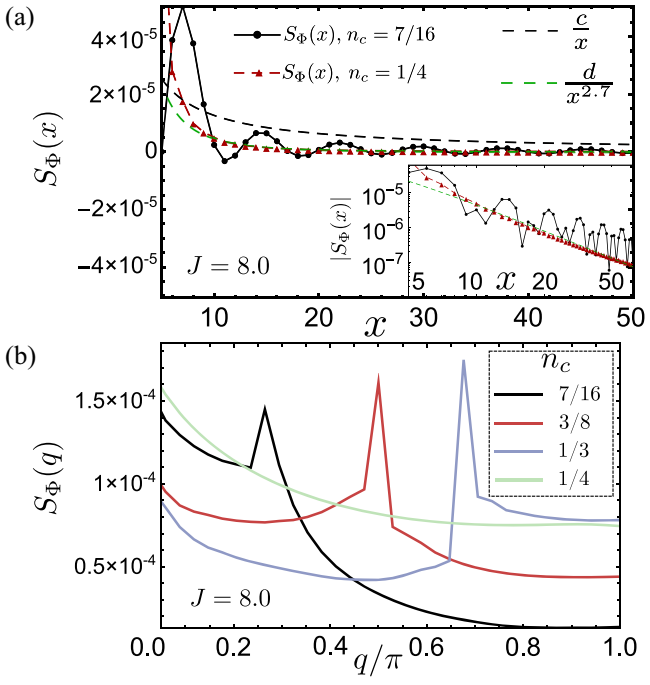

FIG. 4. The nonlocal order parameter $\vec{\Phi}$ captures interference between neighboring hastatic spinors. (a) $S_\Phi(x)$ correlator at $J = 8.0$, $n_c = 1/4$ (insulating HDW) and 7/16 (HDW). There is a clear power-law dependence, with a smaller magnitude than S_Ψ. In metallic regions, S_Φ shows $1/x$ behavior with a clear oscillation. In the insulator, S_Φ is uniform, with a subleading $1/x^\alpha$ power law [39]; we fit $\alpha = 2.7$ for $x \geq 20$. $\vec{\Phi}$ is not present for large N and indicates RKKY physics. Inset: log-log plot confirming power-law decay; $n_c = 1/4$ has a steeper slope than $n_c = 7/16$, due to differing exponents. (b) The Fourier transform $S_\Phi(q)$ for several n_c, $J = 8.0$. $n_c = 1/4$ only has a $Q = 0$ peak, but other fillings show both uniform and oscillating components, with the same Q as S_Ψ.

which must arise from RKKY interactions beyond large N. The correlations shown in Fig. 4 are consistent with simple Landau arguments [39] predicting uniform and Q-modulated components of $\vec{\Phi}$, given a modulated $\vec{\Psi}(Q)$. Away from quarter filling, S_Φ has $1/x$ correlations, with the leading Q vector matching $\vec{\Psi}$, and a potential uniform component. At quarter filling, $\vec{\Phi}$ is uniform, with a distinct subleading $1/x^\alpha$ power law; $\alpha \approx 3$, but is sensitive to the x fitting range, with $\alpha \in \{2.5, 3.5\}$.

To conclude, we find hastatic correlations to be nearly ubiquitous for strong coupling, and have shown that these regions are heavy TLLs whose Fermi surfaces can be understood within large N. The two-channel Kondo insulator at $n_c = 1/4$ is particularly robust, which is relevant for its predicted Majorana zero modes [68]. We also find a predicted hastatic order parameter associated with intersite spinorial interference, which implicates RKKY physics, and signatures of a residual critical nature of the TLL: in the FMHDW, the charge Luttinger parameter K decreases as J increases, meaning the residual interactions are *increasingly* repulsive approaching strong coupling [58], opposite to the single-channel case [9,17]. Further work is needed to resolve $K(J)$ in the HDW and to address whether higher dimensional hastatic phases are non-Fermi liquids [21–23].

We acknowledge stimulating discussions with Bryan Clark, Eduardo Miranda, and Victor L. Quito. This work was primarily supported by the U.S. Department of Energy, Office of Science, Basic Energy Sciences, under Award No. DE-SC001589; central charge calculations were added later and supported by the U.S. DOE, Basic Energy Sciences, Materials Science and Engineering.

[1] N. Read and D. M. Newns, J. Phys. C **16**, 3273 (1983).
[2] P. Coleman, Phys. Rev. B **28**, 5255 (1983).
[3] S. Doniach, Physica (Amsterdam) **91B+C**, 231 (1977).
[4] G. R. Stewart, Adv. Phys. **66**, 75 (2017).
[5] P. Coleman, *Handbook of Magnetism and Advanced Magnetic Materials* (Wiley, New York, 2007), Vol. 1, pp. 95–148.
[6] Q. Si and F. Steglich, Science **329**, 1161 (2010).
[7] H. Tsunetsugu, M. Sigrist, and K. Ueda, Phys. Rev. B **47**, 8345 (1993).
[8] N. Shibata, K. Ueda, T. Nishino, and C. Ishii, Phys. Rev. B **54**, 13495 (1996).
[9] N. Shibata, A. Tsvelik, and K. Ueda, Phys. Rev. B **56**, 330 (1997).
[10] H. Tsunetsugu, M. Sigrist, and K. Ueda, Rev. Mod. Phys. **69**, 809 (1997).
[11] J. C. Xavier, E. Novais, and E. Miranda, Phys. Rev. B **65**, 214406 (2002).
[12] J. C. Xavier and E. Miranda, Phys. Rev. B **70**, 075110 (2004).
[13] N. Xie and Y. F. Yang, Phys. Rev. B **91**, 195116 (2015).
[14] S. A. Basylko, P. H. Lundow, and A. Rosengren, Phys. Rev. B **77**, 073103 (2008).
[15] N. Xie, D. Hu, and Y. F. Yang, Sci. Rep. **7**, 11924 (2017).
[16] J. Chen, E. M. Stoudenmire, Y. Komijani, and P. Coleman, Phys. Rev. Res. **6**, 023227 (2024).
[17] I. Khait, P. Azaria, C. Hubig, U. Schollwöck, and A. Auerbach, Proc. Natl. Acad. Sci. U.S.A. **115**, 5140 (2018).
[18] P. Nozières and A. Blandin, J. Phys. **41**, 193 (1980).
[19] V. J. Emery and S. Kivelson, Phys. Rev. B **46**, 10812 (1992).
[20] D. L. Cox and A. Zawadowski, Adv. Phys. **47**, 599 (1998).
[21] M. Jarrell, H. Pang, and D. L. Cox, Phys. Rev. Lett. **78**, 1996 (1997).
[22] K. Inui and Y. Motome, Phys. Rev. B **102**, 155126 (2020).
[23] H. Hu, L. Chen, C. Setty, M. Garcia-Diez, S. E. Grefe, A. Prokofiev, S. Kirchner, M. G. Vergniory, S. Paschen, J. Cano, and Q. Si, arXiv:2110.06182.
[24] P. Coleman, A. M. Tsvelik, N. Andrei, and H. Y. Kee, Phys. Rev. B **60**, 3608 (1999).
[25] R. Flint, M. Dzero, and P. Coleman, Nat. Phys. **4**, 643 (2008).
[26] S. Hoshino and Y. Kuramoto, Phys. Rev. Lett. **112**, 167204 (2014).
[27] P. Chandra, P. Coleman, and R. Flint, Nature (London) **493**, 621 (2013).
[28] S. Hoshino, J. Otsuki, and Y. Kuramoto, Phys. Rev. Lett. **107**, 247202 (2011).
[29] S. Hoshino, J. Otsuki, and Y. Kuramoto, J. Phys. Conf. Ser. **391**, 012155 (2012).
[30] S. Hoshino, J. Otsuki, and Y. Kuramoto, J. Phys. Soc. Jpn. **82**, 044707 (2013).
[31] G. Zhang, J. S. Van Dyke, and R. Flint, Phys. Rev. B **98**, 235143 (2018).
[32] A. Wugalter, Y. Komijani, and P. Coleman, Phys. Rev. B **101**, 075133 (2020).
[33] Y. Ge and Y. Komijani, Phys. Rev. Lett. **129**, 077202 (2022).
[34] Y. Ge and Y. Komijani, Phys. Rev. Res. **6**, 013247 (2024).
[35] J. Moreno, S. Qin, P. Coleman, and L. Yu, Phys. Rev. B **64**, 085116 (2001).
[36] T. Schauerte, D. L. Cox, R. M. Noack, P. G. J. van Dongen, and C. D. Batista, Phys. Rev. Lett. **94**, 147201 (2005).
[37] M. Jarrell, H. Pang, D. L. Cox, and K. H. Luk, Phys. Rev. Lett. **77**, 1612 (1996).
[38] R. Nourafkan and N. Nafari, J. Phys. Condens. Matter **20**, 255231 (2008).
[39] M. Kornjača and R. Flint, arXiv:2012.08511.
[40] D. L. Cox, Phys. Rev. Lett. **59**, 1240 (1987).
[41] D. L. Cox and M. Jarrell, J. Phys. Condens. Matter **8**, 9825 (1996).
[42] T. Yoshida, Y. Machida, K. Izawa, Y. Shimada, N. Nagasawa, T. Onimaru, T. Takabatake, A. Gourgout, A. Pourret, G. Knebel, and J.-P. Brison, J. Phys. Soc. Jpn. **86**, 044711 (2017).
[43] K. Iwasa, K. T. Matsumoto, T. Onimaru, T. Takabatake, J.-M. Mignot, and A. Gukasov, Phys. Rev. B **95**, 155106 (2017).
[44] J. S. Van Dyke, G. Zhang, and R. Flint, Phys. Rev. B **100**, 205122 (2019).
[45] P. Chandra, P. Coleman, and R. Flint, Phys. Rev. B **91**, 205103 (2015).

[46] A. Houghton, N. Read, and H. Won, Phys. Rev. B **35**, 5123 (1987).
[47] P. Coleman and N. Andrei, J. Phys. Condens. Matter **1**, 4057 (1989).
[48] M. E. Brooks-Bartlett, S. T. Banks, L. D. C. Jaubert, A. Harman-Clarke, and P. C. W. Holdsworth, Phys. Rev. X **4**, 011007 (2014).
[49] S. Petit, E. Lhotel, B. Canals, M. Ciomaga Hatnean, J. Ollivier, H. Mutka, E. Ressouche, A. Wildes, M. R. Lees, and G. Balakrishnan, Nat. Phys. **12**, 746 (2016).
[50] A. Vijayvargia, E. M. Nica, R. Moessner, Y.-M. Lu, and O. Erten, Phys. Rev. Res. **5**, L022062 (2023).
[51] Y. Komijani, A. Toth, P. Chandra, and P. Coleman, arXiv:1811.11115.
[52] A. M. Tsvelik and P. Coleman, Phys. Rev. B **106**, 125144 (2022).
[53] S. R. White, Phys. Rev. Lett. **69**, 2863 (1992).
[54] S. R. White, Phys. Rev. B **48**, 10345 (1993).
[55] M. Fishman, S. R. White, and E. M. Stoudenmire, SciPost Phys. Codebases 4, (2022).
[56] G. Vidal, J. I. Latorre, E. Rico, and A. Kitaev, Phys. Rev. Lett. **90**, 227902 (2003).
[57] N. Laflorencie, E. S. Sørensen, M.-S. Chang, and I. Affleck, Phys. Rev. Lett. **96**, 100603 (2006).
[58] See Supplemental Material at http://link.aps.org/supplemental/10.1103/PhysRevLett.133.026503 for the details of the mean-field calculations presented in the main text and additional DMRG data supporting the conclusions.
[59] H.-K. Jin, W. M. H. Natori, and J. Knolle, Phys. Rev. B **107**, L180401 (2023).
[60] N. Andrei and E. Orignac, Phys. Rev. B **62**, R3596 (2000).
[61] J. Voit, Rep. Prog. Phys. **58**, 977 (1995).
[62] P. Coleman, *Introduction to Many-Body Physics* (Cambridge University Press, Cambridge, England, 2015).
[63] E. Eidelstein, S. Moukouri, and A. Schiller, Phys. Rev. B **84**, 014413 (2011).
[64] M. Oshikawa, Phys. Rev. Lett. **84**, 3370 (2000).
[65] T. Hazra and P. Coleman, Phys. Rev. Res. **3**, 033284 (2021).
[66] R. Peters, N. Kawakami, and T. Pruschke, Phys. Rev. Lett. **108**, 086402 (2012).
[67] D. H. Schimmel, A. M. Tsvelik, and O. M. Yevtushenko, New J. Phys. **18**, 053004 (2016).
[68] M. Kornjača, V. L. Quito, and R. Flint, arXiv:2104.11173.